False vacuum Skyrmions revisited

L. R. Livramento[1,*] and Ya. Shnir[1,2,†]

[1]*BLTP, JINR, Dubna 141980, Moscow Region, Russia*

[2]*Institute of Physics, University of Oldenburg, Oldenburg D-26111, Germany*

(Received 12 May 2022; accepted 8 June 2022; published 28 June 2022)

We consider the classical static soliton solutions of the Skyrme model with false vacuum potential. We make use of fully three-dimensional relaxation calculations to construct global energy minimizers in the sectors of topological degrees from $Q = 1$ to $Q = 6$. These solutions may be metastable, they contain a domain of true vacuum inside the core. Further, we explore small regions of negative topological charge density which appear for the Skyrmions of degrees $Q = 3, 5, 6$.

DOI: 10.1103/PhysRevD.105.125019

I. INTRODUCTION

Many nonlinear classical field theories admit solitons; they represent regular spatially localized field configuration with finite energy, see, e.g., [1,2]. One of the celebrated examples are Skyrmions, the topological soliton solutions of the generalized nonlinear sigma model in $(3 + 1)$ dimensions [3,4], for a review see [5–7]. Originally, the Skyrmions were interpreted as nucleons, with identification of the baryon number and the topological charge of the field configuration. This idea acquired popularity in the 1980s when Witten pointed out that, in the limit of infinite number of colors, the Skyrme model can be considered as a low energy QCD effective theory [8,9]. Apart from being a simple example of a relativistic field model, which supports topological solitons, the Skyrme theory attracted a lot of attention due to its relation to the holonomy of the Yang-Mills instantons via the Atiyah-Manton construction [10] and to the Sakai-Sugimoto model of holographic QCD [11]. On the other hand, Skyrmion-type solutions naturally arise in various condensed matter planar systems with intrinsic and induced chirality [12–15].

According to the scaling arguments of the Derrick's theorem [16], a minimal version of the Skyrme model in $(3 + 1)$-dimensional spacetime, which may supports stable topological solitons, should include both the quadratic in derivatives term L_2 and a term of fourth order in the derivatives L_4 (Skyrme term). However, this form is not so good for a candidate model of nuclear physics; in order to make it more phenomenological suitable for description of baryons and pions one has to supplement it with a potential [17–20].

There is a variety of soliton solutions of the Skyrme model constructed numerically over last three decades, starting from pioneering works [21–23]. The simplest Skyrmion of topological degree $Q = 1$ is spherically symmetric, Skyrmions of higher topological degrees may possess much more complicated symmetries, for example the Skyrmion of degree $Q = 3$ is tetrahedrally symmetric, there are configurations with the symmetries of the dihedral group D_n, the extended dihedral groups D_{nh} and D_{nd}, and the icosahedral group I_n. The rational map parametrization, suggested in [23], provides a nice geometric construction which is very successful at capturing most of the features of the Skyrmions.

Interestingly, it was observed that there are tiny domains of negative topological density for tetrahedral $Q = 3$ Skyrmions, but none for $Q = 2, 4$ Skyrmions with higher amount of symmetry [24–26].

Properties of the multisoliton solutions of the Skyrme model strongly depend on the choice of the potential; it yields the asymptotic decay of the field, which defines the character of interaction between the solitons. Even for the model with the usual pion mass term, the increase of the corresponding mass parameter may strongly affect the structure of the multi-Skyrmion configurations [18,27].

The binding energy of the Skyrmions is relatively high; in order to set it into correspondence with the experimentally known binding energies of physical nuclei, a number of modifications of the Skyrme model have been proposed [28–35]. Notably, solitons of the original Skyrme model do not attain the topological bound, which yields a linear relation between the static energy of the solitons and their topological charges Q. To approach this bound one has to modify the model, preserving its topological properties [31–33,36]. An example is a truncated Skyrme model with

*livramento@theor.jinr.ru

†shnir@theor.jinr.ru

only a sixth-order derivative term, which is the topological current density squared, and a potential [31,33], or modifications of the original theory to the form which supports self-dual equations [37–39]. Multisoliton solutions of this reduced model exactly saturate the topological bound; they may interact only elastically and the self-dual multi-Skyrmion configuration resembles the system of liquid drops. Another interesting example is the false vacuum Skyrme model [40], which is an extension of the static version of the self-dual Skyrme model [38] that preserves the original self-dual equations and treats the baryonic density as a self-interacting fluid. Such a theory does not have a physical potential with true and false minima, but its name comes from the fact that its dynamics is reduced to a single second-order differential equation for a fractional power of baryonic density, which coincides with the Coleman's false vacuum problem. A remarkable consequence is that the baryonic density of the topological solutions with lower static energy must have radial symmetry, leading to Skyrme-type radial solutions that reproduce with excellent accuracy the experimental values of radii and binding energies for a very wide range of the mass number.

In order to construct weakly bounded multi-Skyrmion configurations one can consider a combination of the repulsive and attractive potentials [34,41,42], the latter can be represented by the pion mass term or by the double vacuum potential [43,44]. In such a case, the repulsive part of the potential separates the constituents of the configuration that resembles a loosely bound collection of almost isolated spherically symmetric unit charge Skyrmions. Furthermore, various symmetry-breaking potentials were considered to construct half-Skyrmions [45,46].

An interesting possibility is to consider a potential of the Skyrme model, which possesses both true and false vacua [40,47]. Presence of the false vacuum may affect the properties of the solitons: they become metastable [47–49], the collisions of the solitons could induce the decay of the false vacuum [50], and various radiative effects [51]. However, the previous analysis of the multisoliton solutions of the false vacuum Skyrme model was restricted to an effective theory related to the rational map approximation. Therefore, reexamination of the results obtained in the paper [47] seems to be warranted.

In this paper, we will study classically stable multisoliton solutions of the Skyrme model with the false vacuum potential, discussed earlier in [47]. In particular, we investigate Skyrmions of higher degrees and examine the regions of the negative topological charge density, which appear for the solitons of degrees $Q = 3, 5, 6$ and may have an important effect on false vacuum instability.

II. FALSE VACUUM SKYRMIONS

The Skyrme model is a Poincaré invariant, nonlinear $SU(2)$ sigma model field theory. The basic version of the Skyrme Lagrangian includes two terms, $L_2 + L_4$, or explicitly

$$\mathcal{L}_{\text{Skyrme}} = -\frac{1}{2}\text{Tr}(R_\mu R^\mu) + \frac{1}{16}\text{Tr}([R_\mu, R_\nu][R^\mu, R^\nu]), \tag{1}$$

where we used the rescaled energy and length units $f_\pi/(4e)$ and $2/(ef_\pi)$, respectively [52]. The $SU(2)$ Lie algebra valued right current is $R_\mu = \partial_\mu U U^\dagger = R^a_\mu \tau_a$, with τ_a being the Pauli matrices and U is the so-called Skyrme field, which belongs to the $SU(2)$ Lie group. Once we impose that $U(\mathbf{x}, t)$ takes the same matrix value at spatial infinity, thus the Skyrme field becomes a map $U: S^3 \mapsto S^3$ from the compactified coordinate space $\mathbb{R}^3 \cup \{\infty\} \mapsto S^3$ onto the target space S^3. The topological charge Q corresponds to the degree of this map and can be written in the integral representation as

$$Q = -\frac{1}{24\pi^2}\int d^3x \varepsilon_{ijk}\text{Tr}(R_i R_j R_k). \tag{2}$$

The Lagrangian (1) can be supplemented by symmetry breaking potential terms. The simplest choice is the usual pion mass potential

$$V_{\text{mass}} = m^2\text{Tr}(\mathbb{1} - U), \tag{3}$$

it affects the qualitative shape of Skyrmions of higher degrees [18,27]. The dimensionless parameter m is proportional to the mass of linearized excitations of the scalar field associated with the pions.

Hereafter, we are only concerned with static solutions of the Skyrme model, so we consider the energy density

$$\mathcal{E} = -\frac{1}{2}\text{Tr}(R_i R_i) - \frac{1}{16}\text{Tr}([R_i, R_j][R_i, R_j]) + V(U). \tag{4}$$

The potential of the Skyrme model can be adjusted to model various physical effects, for example, to construct Skyrmions with low binding energies, the pion mass term (3) can be supplemented with an additional term proportional to $\text{Tr}(\mathbb{1} - U)^4$ [41]. Another interesting possibility is to consider a false vacuum potential [47]

$$V = -\frac{1}{4}[m_1^2\text{Tr}(\mathbb{1} - U) + m_2^2\text{Tr}(\mathbb{1} - U^2)], \tag{5}$$

where $U = \mathbb{1}$ is the true vacuum. Therefore, the theory (4) has an $SO(3)$ isospin symmetry corresponding to the field transformation $U \to OUO^{-1}$, $\forall\, O \in SU(2)$. If $U \to -\mathbb{1}$ as $\mathbf{x} \to \infty$, then the following potential shift by m_1^2 is essential

$$V \to V - m_1^2 \underset{\mathbf{x}\to\infty}{\longrightarrow} 0. \tag{6}$$

Below, we assume that the Skyrme field asymptotically may approach both the true and the false vacuum. In the

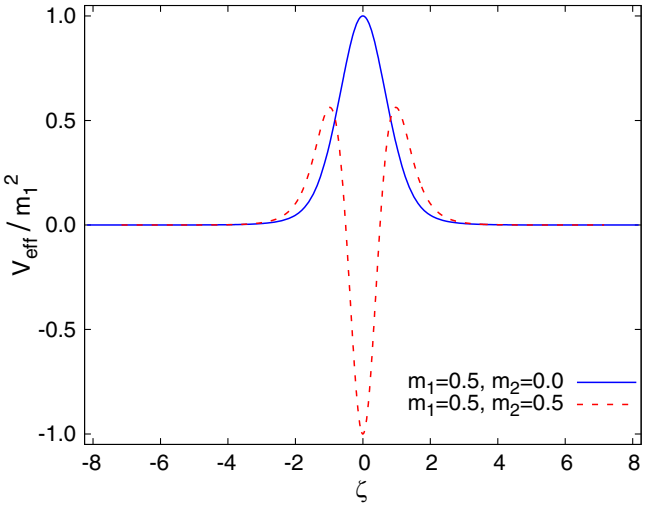

FIG. 1. The effective potential, obtained from the 3D simulations, plotted against ζ for the true vacuum $Q = 1$ Skyrmions at $m_1 = 0.5$ and $m_2 = 0$ and for the false vacuum $Q = 1$ Skyrmions at $m_1 = 0.5$ and $m_2 = 0.5$.

latter case the Skyrmions contain the true vacuum in their core. For later convenience we can introduce an effective potential (see Fig. 1)

$$V_{\rm eff} \equiv \begin{cases} V, & U(\infty) = +\mathbb{1}\ \text{(Skyrmions)} \\ V - m_1^2, & U(\infty) = -\mathbb{1}\ \text{(False vac Skyrmions)} \end{cases}. \tag{7}$$

Note that the potential (5) may possess a local minimum $U_{\rm false} = -\mathbb{1}$ if and only if $m_1^2 < 4m_2^2$. For $m_1^2 \geq 4m_2^2$ the field configuration $U = -\mathbb{1}$ is a global maximum. It is not difficult to check if it expands the $SU(2)$ matrix-valued Skyrme field $U = \mathbb{1}\phi_0 + i\phi_a\tau_a$, where the quartet (ϕ_0, ϕ_a) parametrizes the unit sphere S^3. Then the constraint $\phi_a^2 = 1 - \phi_0^2$ allows us to express the potential (5) as a polynomial of ϕ_0 and find its extrema.

The variation of the Lagrangian of the Skyrme model with the potential term (5) with respect to the field U, after some algebra yields the field equations

$$0 = \partial_\mu\left(R^\mu + \frac{1}{4}[R_\nu, [R^\nu, R^\mu]]\right) + \frac{1}{8}m_1^2(U - U^\dagger) + \frac{m_2^2}{4}(U^2 - U^{\dagger 2}). \tag{8}$$

The asymptotic analysis of the Skyrme field becomes more simple if we make use of the expansion $U = \mathbb{1}\phi_0 + i\phi_a\tau_a$, it yields

$$R_\mu = i\tau_a(\phi_0\partial_\mu\phi_a - \phi_a\partial_\mu\phi_0 + \varepsilon_{abc}\partial_\mu\phi_b\phi_c). \tag{9}$$

Further, we consider excitations v_0, v_a of the Skyrme field around the vacua, $U \sim (-1)^l(1 - v_0)\mathbb{1} + iv_a\tau_a$. Here $|v_0|, |v_a| \ll 1$, and the value of the parameter $l = 0$ corresponds to the asymptotic value of the Skyrme field $U \underset{\mathbf{x}\to\infty}{\longrightarrow} \mathbb{1}$, and $l = 1$ corresponds to the false vacuum asymptotic, $U \underset{\mathbf{x}\to\infty}{\longrightarrow} -\mathbb{1}$ (if $m_1^2 < 4m_2^2$).

Note that although the v_a fields can take both positive and negative values, the v_0 component must be positive due to the constraint of the field to the unit sphere. On the other hand, this constraint yields $v_a^2 = 1 - (1 - v_0)^2$, and since $v_0 \ll 1$, we obtain $v_a^2 \approx 2v_0 + \mathcal{O}(v_0^2)$. Hence, $\partial_i v_0 \approx v_a\partial_i v_a + \mathcal{O}(v_0^2, v_0\partial_i v_0)$. Therefore, $v_0 \ll v_a^2$ and after some algebra we arrive to the linearized form of the field equation (8):

$$\partial_\mu\partial^\mu v_a + m_{\rm eff}^2(l)v_a = 0, \tag{10}$$

where $m_{\rm eff}(l)$ is an effective mass parameter defined by

$$m_{\rm eff}(l) \equiv \sqrt{m_2^2 + (-1)^l\frac{m_1^2}{4}}, \qquad l \equiv \begin{cases} 0, & U(\infty) = +\mathbb{1} \\ 1, & U(\infty) = -\mathbb{1} \end{cases}. \tag{11}$$

Note that the scalar field component ϕ_0 always remain massless while all ϕ_a fields have the same effective mass, which in turn can take on pure real or imaginary values. Evidently, if the Skyrme field asymptotically approached the true vacuum ($l = 0$), then the equation (10) corresponds to the usual Klein-Gordon equation and the triplet of pions has the same non-negative effective mass $m_{\rm eff}^{\text{true vac}} = \sqrt{m_2^2 + \frac{m_1^2}{4}}$. In the massless limit ($m_1^2 = m_2^2 = 0$) the asymptotic triplet of pion fields represent the field of three mutually orthogonal scalar dipoles, $v_a \propto r^{-2}$, see, e.g., [1,2].

For the false vacuum Skyrmions we have to consider three possibilities. First, for $m_{\rm eff}(l = 1) = 0$ the pion excitations are massless, as in the usual minimal Skyrme model without a potential. However, the asymptotic value of the Skyrme field $U \to -\mathbb{1}$ now corresponds to a local maximum of the potential (5): if such a massless configuration contains a bubble of the true vacuum in the interior region, then the solutions may be unstable.

Second, as $m_{\rm eff}^2(l = 1) < 0$, the potential (5) also possesses a global maximum at $U = -\mathbb{1}$, in such a case the linearized equation (10) corresponds to the excitations with purely imaginary mass, i.e., the false vacuum configuration is unstable, the domain of the true vacuum exponentially grows. Third, as $m_{\rm eff}^2(l = 1) > 0$, the linearized equation (10) describes the triplet of massive pions with the same effective mass $m_{\rm eff}^{\text{false vac}} = \sqrt{m_2^2 - \frac{m_1^2}{4}}$. This is probably the most interesting case: if the corresponding false vacuum Skyrmions are metastable, then they can be destroyed via quantum tunneling [53,54] although the decay may be strongly suppressed.

III. THE RATIONAL MAP ANSATZ

Numerical simulations reveal that Skyrmions of higher degrees are not spherically symmetric, they possess very geometrical shapes [21–23]. Rational map approximation [23] gives surprisingly good approximations to the exact numerical solutions. The idea of the rational map ansatz is to map the spheres S^2 centered at the origin of domain space $\mathbb{R}^3$ onto the spheres S^2 that correspond to latitudes in the sphere S^3, the group space of the Skyrme model [23]. Explicitly, let us consider decomposition of the $SU(2)$ group element U in terms of a real valued profile function f and a complex valued function u [1,23,39,55]

$$U = \mathbb{1}\cos f + \frac{i\sin f}{1+|u|^2}\begin{pmatrix} 1-|u|^2 & -2iu \\ 2i\bar{u} & -1+|u|^2 \end{pmatrix}. \quad (12)$$

The scalar components of the Skyrme field $U = \mathbb{1}\phi_0 + i\phi_a\tau_a$ can be written as

$$\phi_0 = \cos f, \qquad \phi_1 = \sin f\,\frac{\bar{u}+u}{1+|u|^2},$$
$$\phi_2 = \sin f\,\frac{i(\bar{u}-u)}{1+|u|^2}, \qquad \phi_3 = \sin f\,\frac{1-|u|^2}{1+|u|^2}. \quad (13)$$

A point on the domain space $\mathbb{R}^3$ can be written in polar coordinates $(r, z, \bar{z})$ on the sphere S^3, where r is the usual radial coordinate, $z = \tan(\theta/2)e^{i\varphi}$ and the metric is given by

$$ds^2 = dr^2 + \frac{4r^2}{(1+|z|^2)^2}dzd\bar{z}. \quad (14)$$

The rational map ansatz (12) for the Skyrme field then can be written as [23]

$$u = u(z) \quad \bar{u} = \bar{u}(\bar{z}), \qquad f = f(r), \quad (15)$$

where $u(z) = p(z)/q(z)$ is a holomorphic rational map between the Riemann spheres S^2, and $p(z)$, $q(z)$ are polynomials of z with no common roots. A well-known property of the rational map is that its algebraic degree, which corresponds to the highest degree among the polynomials $p(z)$ and $q(z)$, is equal to the topological degree of the map u. It can be written in the integral representation as

$$\deg\, u = \frac{1}{4\pi}\int_{S^2} d\Omega\,\vartheta = \max\{\deg p(z), \deg q(z)\}, \quad (16)$$

where $\vartheta(z,\bar{z}) \equiv \left(\frac{1+|z|^2}{1+|u|^2}\right)^2 \frac{du}{dz}\frac{d\bar{u}}{d\bar{z}}$ and we introduced the differential solid angle

$$d\Omega = \sin\theta d\theta \wedge d\psi = \frac{2idz\wedge d\bar{z}}{(1+|z|^2)^2}.$$

The corresponding topological charge density $\mathcal{Q}$ and topological charge (2) associated with the Skyrme field (12) are, respectively,

$$\mathcal{Q} = -\frac{f'\sin^2 f}{2\pi^2 r^2}\vartheta, \qquad Q = \left[\frac{f-\frac{1}{2}\sin(2f)}{\pi}\right]_{r=\infty}^{r=0} \deg\, u, \quad (17)$$

where we used (15) and the definition (16). Therefore, the boundary conditions on the true vacuum configurations are $f(0) = \pi$ and $f(\infty) = 0$, while for the false vacuum Skyrmions we have to impose $f(0) = 2\pi$ and $f(\infty) = \pi$. In both cases the topological degree of the rational map is equal to the topological charge, i.e., $Q = \deg\, u$. However, the false vacuum Skyrmion contains a domain of true vacuum in its center, and the configuration is classically stable [47].

The angular part of the topological charge density (17) can be written alternatively as $\vartheta = \frac{(1+|z|)^2}{(|p|+|q|)^2}|W(z)|^2$, where we introduced the Wronskian

$$W(z) \equiv q(z)p'(z) - p(z)q'(z), \quad (18)$$

which is a polynomial with maximum degree $2(Q-1)$. It so follows that the topological charge density vanishes at the roots of the Wronskian, which, due to $z = \tan(\theta/2)e^{i\varphi}$, corresponds to angular directions. Indeed, although such result is obtained in the rational map approximation, its shed light on why the isosurfaces of topological charge density of the Skyrmions possesses $2(Q-1)$ holes, at least for small values of Q [1].

The rational map ansatz (12), (15) yields the simple radial energy functional normalized by the usual factor $12\pi^2$

$$E = \frac{1}{3\pi}\int_0^\infty dr\Big(r^2 f'^2 + 2Q(f'^2+1)\sin^2 f + \mathcal{I}\frac{\sin^4 f}{r^2} + r^2 V_{\text{eff}}(f)\Big), \quad (19)$$

where $\mathcal{I}$ is the angular integral

$$\mathcal{I} = \frac{1}{4\pi}\int\left(\frac{1+|z|^2}{1+|u|^2}\left|\frac{du}{dz}\right|\right)^4 \frac{2idzd\bar{z}}{(1+|z|^2)^2}.$$

For the spherically symmetric $Q = 1$ Skyrmion $u = z$ and $\mathcal{I} = 1$, while for Skyrmions of higher degrees $1 < B \leq 22$ the best approximation to the global minima is given by the rational map (12) with (see, e.g., [1])

$$\mathcal{I} \approx 1.28 Q^2. \tag{20}$$

Note that in the energy functional (19) for the false vacuum Skyrmions we used the shifted potential (6), as described above.

$$V_{\text{eff}} = V - m_1^2, \qquad V = m_1^2 \sin^2\left(\frac{f}{2}\right) + m_2^2 \sin^2 f. \tag{21}$$

The corresponding variational equation on the profile function f is

$$0 = \sin(2f)\left(Q(f'^2 - 1) - \frac{\mathcal{I}\sin^2 f}{r^2}\right) - \frac{r^2}{2}\frac{\delta V_{\text{eff}}}{\delta f} + (r^2 + 2Q\sin^2 f)f'' + 2f'r. \tag{22}$$

The components of the pion triplet given in (13) has the form $\phi_a = \sin f(r)\varphi_a(z,\bar{z})$, for $a = 1, 2, 3$, where $\varphi_a(z,\bar{z})$ represents the angular dependence, which clearly decouples from the radial part. Asymptotically, we can write the perfil function as $f = l\pi + g$, where the g field is an excitation of the vacuum ($l = 0$) or the false vacuum ($l = 1$). Therefore, the fluctuations of the pion fields are of the form $v_a = (-1)^l g(r)\varphi_a(z,\bar{z})$ (see Sec. II). Hence, the asymptotic equation (10) becomes

$$r^2 g'' + 2rg' - (r^2 m_{\text{eff}}^2(l) + 2\vartheta(z,\bar{z}))\quad g = 0, \tag{23}$$

where we make use of the relation $\partial_i^2 = \frac{(1+|z|^2)^2}{r^2}\partial_{z\bar{z}} + \partial_r^2 + \frac{2}{r}\partial_r$, which follows from the explicit form of the Riemanian metric (14), and $\partial_{z\bar{z}}\varphi_a = -\frac{2\partial_z u \partial_{\bar{z}}\bar{u}}{(1+|u|^2)^2}\varphi_a$. Note that the angular dependent term $\varphi_a(z,\bar{z})$ in the radial asymptotic equation (10) is always decoupled.

Multiplying the equation (23) by $\frac{1}{4\pi}d\Omega$, integrating over the S^2 and using (16), we obtain the radial asymptotic equation

$$r^2 g'' + 2rg' - (r^2 m_{\text{eff}}^2(l) + 2Q)g = 0. \tag{24}$$

Note that, for $m_{\text{eff}}(l) = 0$, the potential term vanishes both for the true and false vacuum Skyrmions, the radial function $g(r)$ decays asymptotically as $g \propto a/r^2$ and in both cases the asymptotic triplet of pion fields represents the field of three mutually orthogonal scalar dipoles. Equation (24) can be obtained alternatively considering the asymptotic regime of (22) with $f = l\pi + g$.

Clearly, the energy of the false vacuum Skymions diverge as $m_{\text{eff}}^2(l) = m_2^2 - m_1^2/4 < 0$ and the effective mass parameter in the asymptotic Klein-Gordon equation (24) becomes purely imaginary.

IV. NUMERIC SOLUTIONS

To find stationary points of the energy functional (4) we implement the simulated annealing technique [56] numerically relaxing initial field configurations, produced by the rational map approximation in a sector of topological degree Q. As a consistency check, we verify that our algorithm correctly reproduces the known results for the Skyrmion configurations of the usual rescaled Skyrme model with pion mass potential (3), for degrees up to $Q = 6$ it agrees with previously known values of the ratio E/Q within 1.0% accuracy. For each solution we evaluated the value of the topological charge Q, we find that this is accurate to within 10^{-3} in all simulations reported here. Another check of the correctness of our results was performed by verifying that the virial relation for the Skyrme model in $3+1$ dimensions between the potential, quadratic, and quartic in derivatives terms in the static energy functional, $E_2 = E_4 - 3E_0$ is satisfied. Here

$$E_0 \equiv \frac{1}{12\pi^2}\int d^3x\, V_{\text{eff}}, \qquad E_2 \equiv \frac{1}{24\pi^2}\int d^3x\, \text{Tr}(R_i R_i),$$
$$E_4 \equiv \frac{1}{192\pi^2}\int d^3x\, \text{Tr}([R_i, R_j][R_i, R_j]). \tag{25}$$

More precisely, following the discussion of the loosely bounded Skyrmions presented in [41], we evaluated the quantity

$$\mathcal{D} = \frac{E_4 - E_2 - 3E_0}{E_4 + E_2 + E_0} \tag{26}$$

for each solution we found. In order to have a measure of the characteristic size of Skyrmions we also introduce the root mean square (rms) radius defined by

$$\sqrt{\langle r^2\rangle} \equiv \sqrt{\frac{1}{Q}\int d^3x\, r^2 \mathcal{Q}}. \tag{27}$$

Note that using the virial identity we can also estimate the accuracy of the rational map approximation (15) for which

$$E_2 = \frac{1}{3\pi}\int_0^\infty dr(r^2 f'^2 + 2Q\sin^2 f),$$
$$E_4 = \frac{1}{3\pi}\int_0^\infty dr\left(2Qf'^2\sin^2 f + \mathcal{I}\frac{\sin^4 f}{r^2}\right),$$
$$E_0 = \frac{1}{3\pi}\int_0^\infty dr\, r^2 V_{\text{eff}}(f). \tag{28}$$

We found that the virial constraint is satisfied with an accuracy of order of 10^{-2} for all solutions considered in this paper.

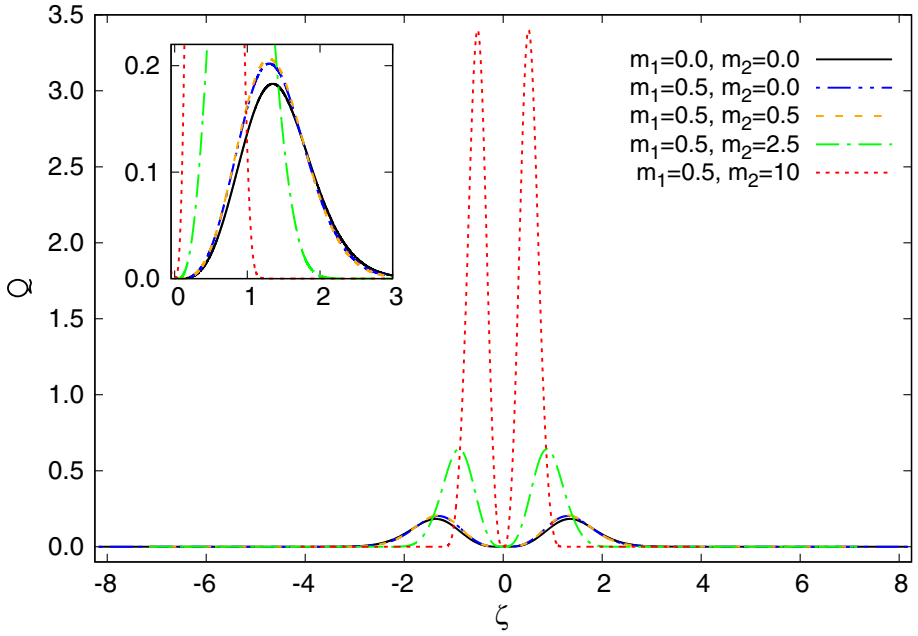

FIG. 2. The topological charge density $\mathcal{Q}$ plotted against ζ for the true vacuum Skyrmions at $m_1 = 0$, 0.5, $m_2 = 0$ and for the corresponding false vacuum Skyrmions at $m_1 = 0.5$ and some set of values of m_2.

The results presented here used cubic grids containing 120^3 points and Dirichlet boundary conditions (10) are imposed, i.e., we set $U = (-1)^I \mathbb{1}$ at the edge of the lattice. The spatial grid spacing is $\Delta x = 0.08$, and consequently the spacial grid size is $R = 9.52$. Smaller grid spacing was used to study specific domains of negative values of the topological charge densities. For comparison we also solved one-dimensional radial equation for the $Q = 1$ spherically symmetric Skyrmion on the grid with spacing $\Delta x = 0.005$ and 4001 points, the errors in evaluation of the topological degree are less than 0.1%.

A. False vacuum Skyrmions

First, we considered multisoliton solutions of the Skyrme model with the false vacuum potential (5) we discussed above. While the previous consideration of this system in [47] was restricted to the rational map ansatz with the approximation (20), even for the Skyrmions of very high degrees, we perform full 3D numerical computations to find corresponding global minima. Evidently, these configurations do not possess spherical symmetry, the false vacuum Skyrmions have an effective mass $m_{\text{eff}} \equiv \sqrt{m_2^2 - \frac{m_1^2}{4}}$ and the binding energy of these Skyrmions is large. We found that the rational map approximation yields a very good initial approximation both for the true vacuum Skyrmions with the usual pion mass potential (3) and for the false vacuum Skyrmions with the potential (5).

The distributions of the energy and topological charge density of the false vacuum Skyrmions depend on the effective potential (7) which depends both on m_1 and m_2 and defines the corresponding pressure and shear forces inside the configuration. As an example, Figs. 2 and 3 display plots of the topological charge density on the diagonal line through the center of the $Q = 4$ configuration and the profiles of scalar component ϕ_0 for some set of values of the parameters m_1, m_2. Such line corresponds to the points where all Cartesian coordinates (x_1, x_2, x_3) are equal, which can be easily parametrized by $\zeta \equiv \text{sign}(x_1)r$. The results of our simulations are presented in Tables I–III and Figs. 4 and 5.

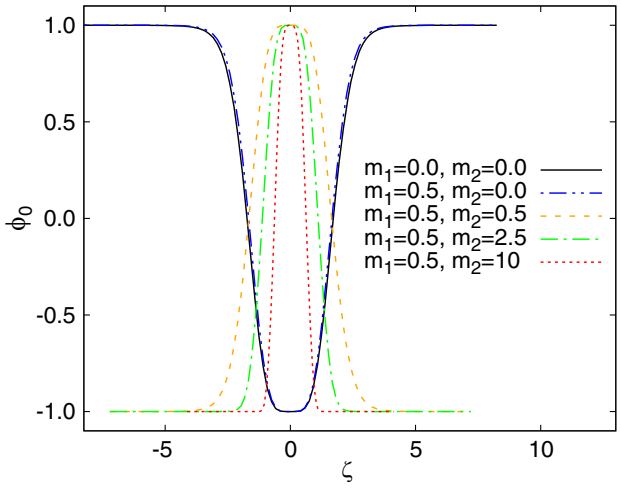

FIG. 3. The profile of the scalar component ϕ_0 of the field of $Q = 4$ Skyrmion plotted against ζ for the true vacuum Skyrmions at $m_1 = 0$, 0.5, $m_2 = 0$, and for the false vacuum $Q = 4$ Skyrmions at $m_1 = 0.5$ and some set of values of m_2.

TABLE I. False vacuum Skyrmions at $m_1 = 0.5$, $m_2 = 0.5$ with topological charges $Q = 1$–6: Numerically computed values of the ratio E/Q, Derrick constraint (26), the rms radius (27) and the values of the static energy E and the topological degree Q (numerical) evaluated in full 3D numerical simulations. In addition, the first row records the data for the spherically symmetric Skyrmion $Q = 1^*$ on 1D grid with 4001 points and lattice spacing $\Delta x = 0.005$.

Q	E/Q	$\mathcal{D}$	$\sqrt{\langle r^2\rangle}$	E	Q (numerical)
1^*	1.2716	−0.0016	0.9655	1.2716	1.0000
1	1.2761	0.0213	0.9510	1.2770	1.0007
2	1.2146	0.0155	1.3204	2.4308	2.0014
3	1.1761	0.0186	1.5510	3.5301	3.0015
4	1.1464	0.0219	1.7355	4.5885	4.0024
5	1.1426	0.0282	1.9343	5.7163	5.0028
6	1.1317	0.0322	2.0830	6.7939	6.0033

TABLE II. False vacuum Skyrmions, the same quantities as those given above in Table I for $m_1 = 0.5$, $m_2 = 2.5$.

Q	E/Q	$\mathcal{D}$	$\sqrt{\langle r^2\rangle}$	E	Q (numerical)
1^*	1.6384	0.0001	0.6288	1.6384	1.0000
1	1.6381	−0.0025	0.6332	1.6406	1.0015
2	1.5591	−0.0025	0.8764	3.1228	2.0029
3	1.5075	−0.0020	1.0259	4.5277	3.0034
4	1.4650	−0.0022	1.1507	5.8679	4.0053
5	1.4588	−0.0021	1.2870	7.3031	5.0063
6	1.4425	−0.0021	1.3899	8.6658	6.0074

TABLE III. False vacuum Skyrmions, the same quantities as those given above in Table I for $m_1 = 0.5$, $m_2 = 10$.

Q	E/Q	$\mathcal{D}$	$\sqrt{\langle r^2\rangle}$	E	Q (numerical)
1^*	2.6055	0.0000	0.3609	2.6055	1.0000
1	2.6047	−0.0022	0.3634	2.6086	1.0015
2	2.4920	−0.0020	0.5023	4.9907	2.0027
3	2.4233	−0.0017	0.5821	7.2791	3.0038
4	2.3601	−0.0018	0.6489	9.4520	4.0048
5	2.3528	−0.0015	0.7236	11.7784	5.0061
6	2.3293	−0.0015	0.7786	13.9929	6.0074

Figure 4 demonstrates that the energies of the $Q = 1$–6 false vacuum Skyrmions increases approximately linearly with Q, which is expected since the binding energy per topological charge unit $E_B \equiv E_{Q=1} - E_Q/Q$ is about 5–10% of $E_{Q=1}$ for $Q > 1$ (see Tables I–III). However, one can expect this pattern may change for Skyrmions of higher degrees [18,27]. Dependency of the ratio E/Q of these configurations on the effective mass m_{eff} is displayed in Fig. 5. By analogy with the corresponding curves in the model with the usual pion mass potential (3), it increases with m_{eff}.

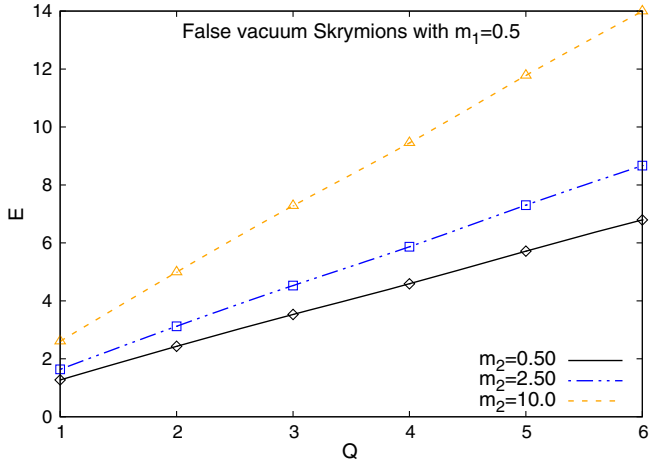

FIG. 4. The values of energy E of the false vacuum Skyrmions, presented in the Tables I–III, plotted against Q.

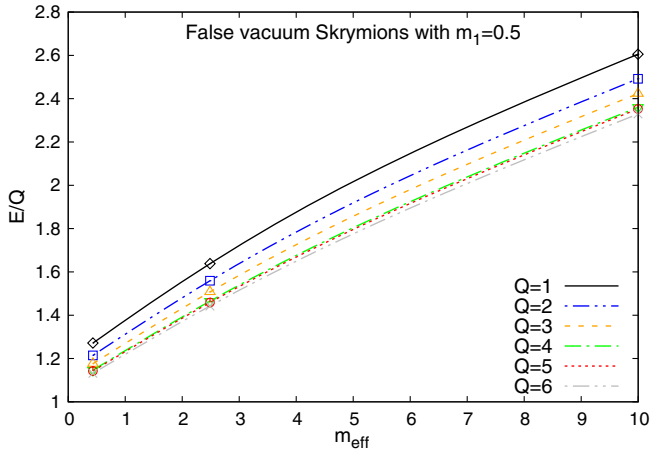

FIG. 5. The values of the energy per topological charge E/Q of the false vacuum Skyrmions, presented in the Tables I–III, plotted against the effective mass $m_{\text{eff}} \equiv \sqrt{m_2^2 - \frac{m_1^2}{4}}$.

It is instructive to visualize the solutions of the model (4) by displaying 3D isosurfaces of the topological charge densities $\mathcal{Q}$, see, e.g., [1]. However, variation of the mass parameter significantly affects the characteristic size of the field configuration. In our simulations, for each solution we found numerically on a discretized 3D grid, we introduce an α function, which is defined as a sum of the edges of the elementary parallelepiped in the domain of the lattice that contains an isosurface of the topological density. Explicitly, α is a function of m_1, m_2, l, $\mathcal{Q}$, and Q, i.e., $\alpha = \alpha(Q, m_1, m_2, l, \mathcal{Q})$. Using this function, we can scale an isosurface of the topological density plotted for some value of the density $\mathcal{Q}$, to make a visual correspondence with a different plot for another value of $\mathcal{Q}$. In other words, we can define a "zoom factor" between the

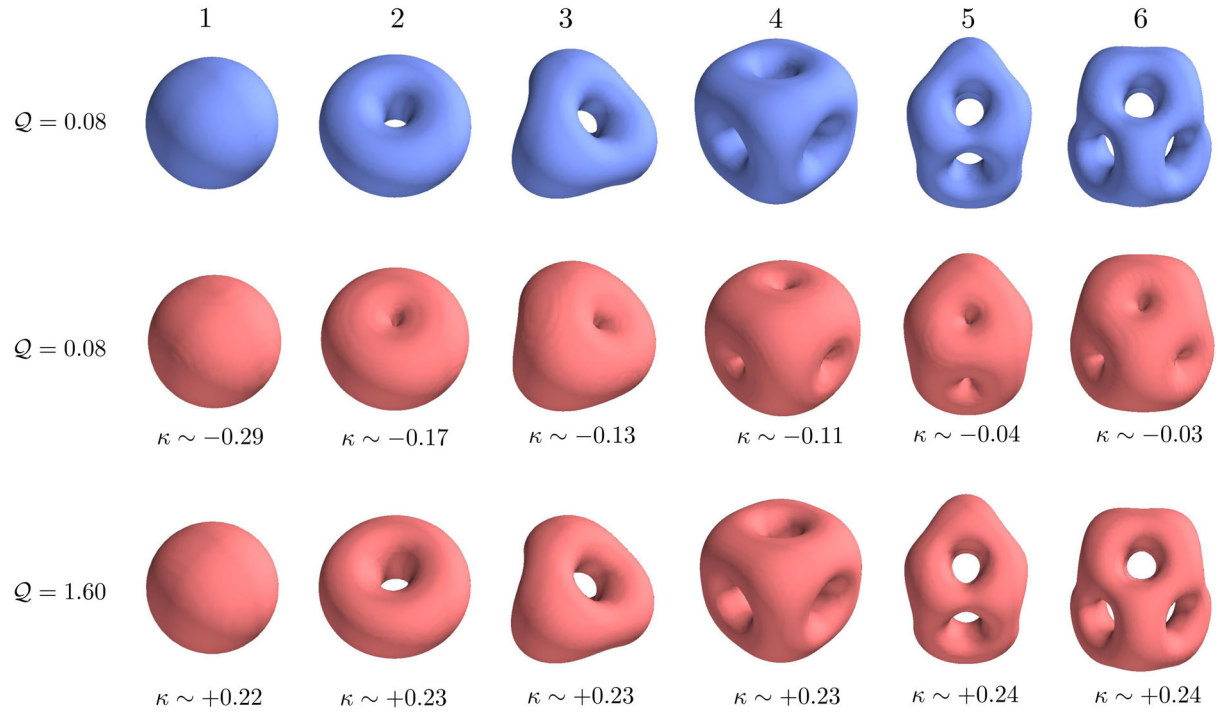

FIG. 6. Three sets of charge density isosurfaces of the Skyrmions degrees $Q = 1$ to $Q = 6$, from left to right. The upper row displays the true vacuum massive Skyrmions (blue figures) for $m_1 = 0.5$ and $m_2 = 0$ at $\mathcal{Q} = 0.08$. The second and the third rows displays false vacuum Skyrmions (red figures) for $m_1 = 0.5$ and $m_2 = 10$ at $\mathcal{Q} = 0.08$ and $\mathcal{Q} = 1.6$, respectively, rescaled to be approximately the same size. The factor κ is defined by (29).

corresponding isosurfaces of the topological charge densities as, for example,

$$\kappa(Q, m_2, \mathcal{Q}) \equiv 1 - \frac{\alpha(Q, 0.5, m_2, 1, \mathcal{Q})}{\alpha(Q, 0.5, 0, 0, 0.08)}, \qquad (29)$$

where, as a reference point, we used the function $\alpha(Q, 0.5, 0, 0, 0.08)$, and it corresponds to the usual massive Skyrmions with $m_1 = 0.5$.

Figure 6 displays the corresponding rescaled isosurfaces of the charge densities for the usual true vacuum massive Skyrmions (blue figures, upper row) for $m_1 = 0.5$ and $m_2 = 0$, and the false vacuum Skyrmions (red figures, middle and bottom rows) for $m_1 = 0.5$ and $m_2 = 10$, respectively. Clearly, geometrical shapes of the global minimizers in the Skyrme model with the true vacuum potential (3) and with the false vacuum potential (5) are very similar.

V. REGIONS OF NEGATIVE TOPOLOGICAL CHARGE DENSITY

A peculiar feature of the Skyrmions is that they allow for existence of regions of negative topological charge density [24,25]. It was argued that these regions are associated with singularities of the nonholomorphic rational map, this conjecture was supported by direct numerical simulations for the tetrahedrally symmetric minimum-energy $Q = 3$ Skyrmion [25]. It was shown that the regions of negative topological charge density of this configurations represent a tiny dual tetrahedron at the center of the configuration, with four small tubes smoothly joining it up and further, passing though the faces of the tetrahedron of positive topological density. It was pointed out that in the model with the usual pion mass term (3), the tubes become more pronounced [25]. It was also verified that $Q = 2$ and $Q = 4$ Skyrmions do not support any regions of negative baryon density [24–26].

Our aim now is to extend this study to the Skyrmions of higher degrees $Q = 5$, 6 also considering the model with false vacuum potential (5). Since the regions of the negative topological density are very tiny, we have to refine our numerical algorithm to truly capture these domains. First, we construct a Skyrmion solution on a lattice with 120^3 points, with spacing $\Delta x \sim 0.08$, and then we select some particular rectangular region of the lattice. Second, we use polynomial three-dimensional interpolation to multiply the number of points inside and at the border of this small sublattice, by typically factor of 4, reducing the lattice spacing, correspondingly. The polynomial expansion of the fields on the new sublattice is used to generate new input data. Finally, we repeat the simulated annealing algorithm inside the new lattice using the fixed boundary conditions. We can repeat this procedure multiple times to investigate very tiny structures, like the regions of the negative topological densities inside the core of the Skyrmions.

TABLE IV. The effective mass $m_{\text{eff}} = \sqrt{m_2^2 + l\frac{m_1^2}{4}}$, the minimal ($\mathcal{Q}_-$) and the maximal ($\mathcal{Q}_+$) values of the topological density for the tetrachedral $Q = 3$ Skyrmions ($l = 1$) and false vacuum Skyrmions ($l = -1$).

Type	m_1	m_2	m_{eff}	$\mathcal{Q}_-$ (10^{-3})	$\mathcal{Q}_+$
Standard $Q = 3$ Skyrmion	0.0	0.0	0.0000	−3.50	0.245
Massive $Q = 3$ Skyrmion	0.5	0.0	0.2500	−3.65	0.255
False $Q = 3$ Skyrmion	0.5	0.5	0.4330	−3.56	0.262
False $Q = 3$ Skyrmion	0.5	2.5	2.4875	−6.99	0.790
False $Q = 3$ Skyrmion	0.5	10.0	9.9969	−15.22	4.036

First, we revisit the $Q = 3$ Skyrmion. Considering the usual model with the pion mass potential (3), we find numerically the dual tetrahedron of negative topological density about the origin, the corners of the tetrahedron are linked to the four tubes [25]. Consequent decrease of the lattice spacing allows us to refine the shapes of these regions, the values of the charge density presented in Table IV are in reasonable agreement with results reported in [25]. Figure 7 displays the isosurfaces of the topological charge density of the $Q = 3$ Skyrmions. Clearly, increase of the resolution reveals a very fine structure of the domains of negative charge density.

For the usual Skyrme model the value of the field is close to the antivacuum, $U \to -\mathbb{1}$ at the center of the configuration, and it is taking the vacuum value on the boundary. For the model with the false vacuum potential (5) the situation is inverse, see Fig. 3. However, the structure of the domains of the negative charge density for the tehrahedral $Q = 3$ Skyrmions remains the same, see Fig. 7. Our numerical results indicate that the presence of the these regions do not destabilize the false vacuum Skyrmions for all ranges of values of the effective mass.

It was pointed out, that the occurrence of the regions of negative topological charge density is related with zeros of the Wronskian (18) associated to the rational map [24,25]. More precisely, the zeros of the distribution of the topological charge density correspond to the folding of the Skyrme field, which is a map between the spheres S^3. It was observed, however, that there is no regions of negative charge density for the axially symmetric $Q = 2$ Skyrmion and for the $Q = 4$ with cubic symmetry [24–26]. Our numerical simulations confirm this result. It was also pointed out [24] that the folding structure of the holomorphic rational map of the $Q = 5$ Skyrmions may give rise to the regions of negative charge density associated with zeros of the Jacobian matrix of the Skyrme map, but this was never observed in numerical calculations.

In order to check this hypothesis numerically, we perform a detailed study of the global minimizers in the sectors of topological degrees $Q = 5$ and $Q = 6$. A best approximation to the D_{2d}-symmetric $Q = 5$ Skyrmion is given by the holomorphic rational map (15)

$$u(z) = \frac{z(z^4 + bz^2 + a)}{az^4 - bz^2 + 1}, \tag{30}$$

where a, b are two real parameters. The rational map is minimized when $a = 3.07$, $b = 3.94$, it yields a polyhedron constructed from four pentagons and four quadrilaterals [57]. Since the Wronskian (18) associated with (30) possesses eight roots, it follows that this map gives rise to eight singular rays, which start at the origin. Our numerical analysis of the minimum energy $Q = 5$ Skyrmion in the

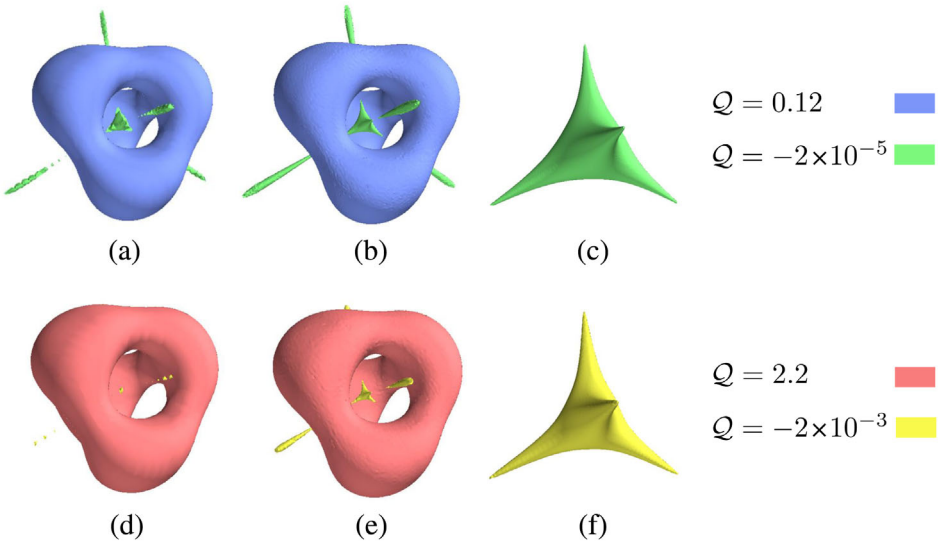

FIG. 7. Isosurfaces of the topological charge density for $Q = 3$ Skyrmions. Upper row: usual massive Skyrme model potential at $m_1 = 0.5$ and $m_2 = 0$. Bottom row: the model with the false vacuum potential (5) at $m_1 = 0.5$ and $m_2 = 10$. The lattice spacing in the simulations for the plots (a)–(c) are $\Delta x = 0.08, 0.02, 0.005$, and for the plots (d)–(e) are $\Delta x = 0.04, 0.01, 0.0025$, respectively.

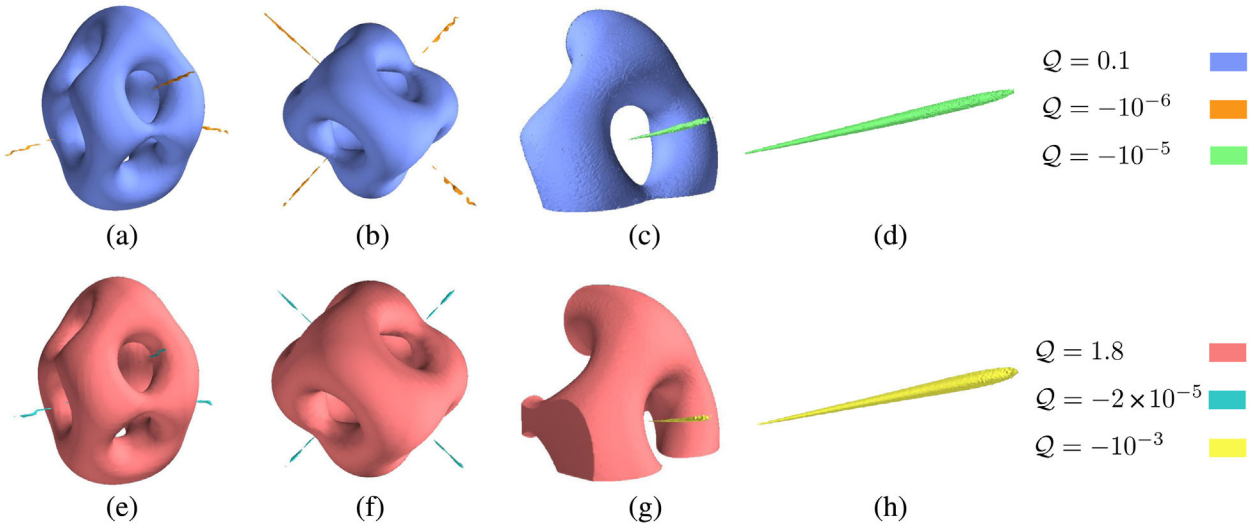

FIG. 8. Isosurfaces of the topological charge density for $Q = 5$ Skyrmions. Upper row: usual massive Skyrme model with the potential (5) at $m_1 = 0.5$ and $m_2 = 0$. Bottom row: the model with the false vacuum potential (5) at $m_1 = 0.5$ and $m_2 = 10$. The lattice spacing in the simulations for the plots (a)–(d) are $\Delta x = 0.08, 0.08, 0.02, 0.005$, and for the plots (e)–(h) are $\Delta x = 0.04, 0.04, 0.01, 0.0025$, respectively. Clearly, we plot only one isosurface of negative topological charge density in each plot.

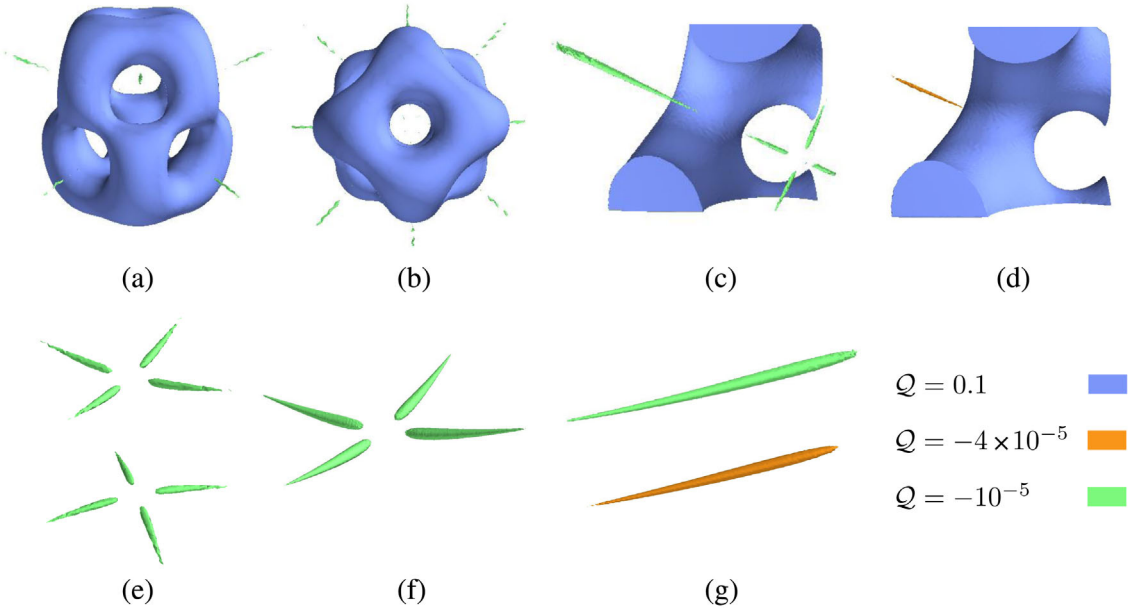

FIG. 9. Isosurfaces of the topological charge density for $Q = 6$ Skyrmions in the usual massive Skyrme model with the potential (5) at $m_1 = 0.5$ and $m_2 = 0$. The lattice spacing in the simulations for the plots from (a)–(g) are $\Delta x = 0.08, 0.08, 0.02, 0.02, 0.02, 0.005, 0.005$, respectively.

model with pion mass potential (3) reveals four tiny regions of negative topological density, see Fig. 8.

The polyhedral $Q = 6$ Skyrmion can be constructed via the D_{4d} symmetric rational map [57]

$$u(z) = \frac{z^4 + a}{z^2(az^4 + 1)},$$

where the parameter of the map has to be taken as $a = 0.16i$ to minimize the energy. This map gives rise to ten singular rays, which start at the origin. The $Q = 6$ configuration can be regarded as a bounded system of two Skyrmions of charges $Q = 4$ and a $Q = 2$, see Figs. 9 and 10. Interestingly, we found eight small tubes of negative charge density, both in the usual Skyrme model and in the model with false vacuum potential (5).

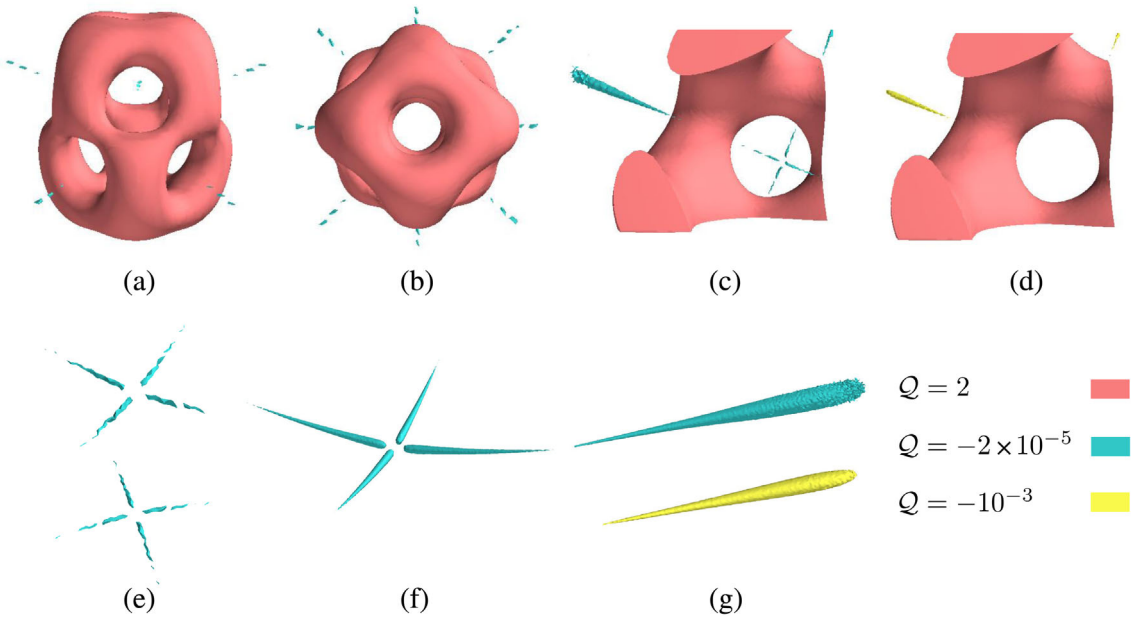

FIG. 10. The isosurfaces of topological charge density of the $Q = 6$ Skyrmions in the model with the false vacuum potential (5) at $m_1 = 0.5$ and $m_2 = 10$. The lattice spacing in the simulations for the figures from (a)–(g) are $\Delta x = 0.04, 0.04, 0.01, 0.01, 0.01, 0.0025, 0.005$, respectively.

VI. CONCLUSION

Our motivation for this study is twofold. On the one hand, we want to extend the analysis of the paper [47], to the global minimizers of the Skyrme model with the false vacuum potential (5). On the other hand, we studied the structure of the small domains of the negative topological charge densities for Skyrmions of degrees higher than three. We have performed fully three-dimensional numerical relaxations of Skyrmions with topological charges from $Q = 1$ to $Q = 6$ both in the Skyrme model with the conventional pion mass term included and in the model with generalized potential (5), which admits false vacuum Skyrmions. The rational map parametrization was used to generate initial data in both models. Our calculations show that, as the effective mass m_{eff} remains positive, the shapes of the soliton solutions in both models are qualitative similar, the effective mass is playing the role of the pion mass parameter. The false vacuum Skyrmions are metastable, they contain a domain of true vacuum inside the core. These configurations are classically stable; however, they can decay via quantum tunneling. On the other hand, the presence of the domains of true vacuum may induce instability of the colliding false vacuum Skyrmions, as compared with scattering of the usual Skyrmions [58]. Similar effect may be observed for classically isorotating Skyrmions [59] and baby Skyrmions [60,61] in the model with a false vacuum potential.

We also explored numerically very small regions of negative topological density which appear for the Skyrmions of degrees $Q = 3, 5, 6$ both in the model with pion mass potential and for the false vacuum Skyrmions. We confirm that these regions are associated with singularities in the rational map ansatz. Our numerical full field simulations verified previous conclusions [24–26] that the regions of negative charge density do not appear for the Skyrmions of degrees $Q = 2$ and $Q = 4$.

Obviously it is important to study the quantum decay rate of the metastable false vacuum Skyrmions. This task may be performed beyond the thin wall approximation by applying advanced numerical methods, see, e.g., [62]. We believe it will be interesting to study if the regions of negative charge density may catalyze the vacuum decay. Extending this analysis to the Skyrmions of higher degrees also can be an interesting problem. Another direction for future study is to consider the extended Skyrme model with sixtic terms [31,63,64] and a false vacuum potential.

ACKNOWLEDGMENTS

Y. S. gratefully acknowledges the support by the Ministry of Education of Russian Federation, Project No. FEWF-2020-003. The computations in this paper were run on the "GOVORUN" cluster supported by the Laboratory of Information Technologies (LIT), Joint Institute for Nuclear Research (JINR).

[1] N. Manton and P. Sutcliffe, *Topological Solitons* (Cambridge University Press, New York, 2004).
[2] Y. M. Shnir, *Topological and Non-Topological Solitons in Scalar Field Theories* (Cambridge University Press, Cambridge, England, 2018).
[3] T. H. R. Skyrme, A nonlinear field theory, Proc. R. Soc. A **260**, 127 (1961).
[4] T. H. R. Skyrme, A unified field theory of mesons and baryons, Nucl. Phys. **31**, 556 (1962).
[5] I. Zahed and G. E. Brown, The Skyrme model, Phys. Rep. **142**, 1 (1986).
[6] G. E. Brown and M. Rho, *The Multifaceted Skyrmion* (World Scientific, Singapore, 2010).
[7] N. Manton, *Skyrmions—A Theory of Nuclei* (World Scientific, Singapore, 2022).
[8] E. Witten, Global aspects of current algebra, Nucl. Phys. **B223**, 422 (1983).
[9] E. Witten, Current algebra, baryons, and quark confinement, Nucl. Phys. **B223**, 433 (1983).
[10] M. F. Atiyah and N. S. Manton, Skyrmions from instantons, Phys. Lett. B **222**, 438 (1989).
[11] T. Sakai and S. Sugimoto, Low energy hadron physics in holographic QCD, Prog. Theor. Phys. **113**, 843 (2005).
[12] A. Bogdanov and D. Yablonskii, Thermodynamically stable "vortices" in magnetically ordered crystals. The mixed state of magnets, Sov. Phys. JETP **68**, 101 (1989).
[13] A. Bogdanov, New localized solutions of the nonlinear field equations, JETP Lett. **62**, 247 (1995).
[14] A. O. Leonov and M. Mostovoy, Multiply periodic states and isolated skyrmions in an anisotropic frustrated magnet, Nat. Commun. **6**, 8275 (2015).
[15] N. Nagaosa and Y. Tokura, Topological properties and dynamics of magnetic skyrmions, Nat. Nanotechnol. **8**, 899 (2013).
[16] G. H. Derrick, Comments on nonlinear wave equations as models for elementary particles, J. Math. Phys. (N.Y.) **5**, 1252 (1964).
[17] G. S. Adkins and C. R. Nappi, The Skyrme model with pion masses, Nucl. Phys. **B233**, 109 (1984).
[18] R. Battye and P. Sutcliffe, Skyrmions and the pion mass, Nucl. Phys. **B705**, 384 (2005).
[19] V. B. Kopeliovich, B. Piette, and W. J. Zakrzewski, Mass terms in the Skyrme model, Phys. Rev. D **73**, 014006 (2006).
[20] S. B. Gudnason and M. Nitta, Modifying the pion mass in the loosely bound Skyrme model, Phys. Rev. D **94**, 065018 (2016).
[21] E. Braaten, S. Townsend, and L. Carson, Novel structure of static multi-soliton solutions in the Skyrme model, Phys. Lett. B **235**, 147 (1990).
[22] R. A. Battye and P. M. Sutcliffe, Symmetric Skyrmions, Phys. Rev. Lett. **79**, 363 (1997).
[23] C. J. Houghton, N. S. Manton, and P. M. Sutcliffe, Rational maps, monopoles and Skyrmions, Nucl. Phys. **B510**, 507 (1998).
[24] C. J. Houghton and S. Krusch, Folding in the Skyrme model, J. Math. Phys. (N.Y.) **42**, 4079 (2001).
[25] D. Foster and S. Krusch, Negative Baryon density and the Folding structure of the $B = 3$ Skyrmion, J. Phys. A **46**, 265401 (2013).
[26] R. A. Leese and N. S. Manton, Stable instanton generated Skyrme fields with baryon numbers three and four, Nucl. Phys. **A572**, 575 (1994).
[27] R. Battye and P. Sutcliffe, Skyrmions with massive pions, Phys. Rev. C **73**, 055205 (2006).
[28] A. Jackson, A. D. Jackson, A. S. Goldhaber, G. E. Brown, and L. C. Castillejo, A modified skyrmion, Phys. Lett. **154B**, 101 (1985).
[29] U. G. Meissner and I. Zahed, Nucleons from Skyrmions with vector mesons, Z. Phys. A **327**, 5 (1987).
[30] L. Marleau, Modifying the Skyrme model: Pion mass and higher derivatives, Phys. Rev. D **43**, 885 (1991).
[31] C. Adam, J. Sanchez-Guillen, and A. Wereszczynski, A Skyrme-type proposal for baryonic matter, Phys. Lett. B **691**, 105 (2010).
[32] P. Sutcliffe, Skyrmions in a truncated BPS theory, J. High Energy Phys. 04 (2011) 045.
[33] C. Adam, C. Naya, J. Sanchez-Guillen, R. Vazquez, and A. Wereszczynski, The Skyrme model in the BPS limit, arXiv:1511.05160.
[34] S. B. Gudnason, B. Zhang, and N. Ma, Generalized Skyrme model with the loosely bound potential, Phys. Rev. D **94**, 125004 (2016).
[35] S. B. Gudnason and M. Nitta, A higher-order Skyrme model, J. High Energy Phys. 09 (2017) 028.
[36] C. Naya and P. Sutcliffe, Skyrmions in models with pions and rho mesons, J. High Energy Phys. 05 (2018) 174.
[37] L. Ferreira and Y. Shnir, Exact self-dual skyrmions, Phys. Lett. B **772**, 621 (2017).
[38] L. Ferreira, Exact self-duality in a modified Skyrme model, J. High Energy Phys. 07 (2017) 039.
[39] L. Ferreira and L. Livramento, Self-duality in the context of the Skyrme model, J. High Energy Phys. 09 (2020) 031.
[40] L. A. Ferreira and L. R. Livramento, A false vacuum Skyrme model for nuclear matter, arXiv:2106.13335v2.
[41] M. Gillard, D. Harland, and M. Speight, Skyrmions with low binding energies, Nucl. Phys. **B895**, 272 (2015).
[42] S. B. Gudnason, Exploring the generalized loosely bound Skyrme model, Phys. Rev. D **98**, 096018 (2018).
[43] C. Adam, C. D. Fosco, J. M. Queiruga, J. Sanchez-Guillen, and A. Wereszczynski, Symmetries and exact solutions of the BPS Skyrme model, J. Phys. A **46**, 135401 (2013).
[44] I. Perapechka and Y. Shnir, Crystal structures in generalized Skyrme model, Phys. Rev. D **96**, 045013 (2017).
[45] J. Jaykka and M. Speight, Easy plane baby skyrmions, Phys. Rev. D **82**, 125030 (2010).
[46] S. B. Gudnason and M. Nitta, Fractional Skyrmions and their molecules, Phys. Rev. D **91**, 085040 (2015).
[47] E. Dupuis, M. Haberichter, R. MacKenzie, M. B. Paranjape, and U. A. Yajnik, Vacuum decay induced by false Skyrmions, Phys. Rev. D **99**, 016016 (2019).
[48] B. Kumar, M. B. Paranjape, and U. A. Yajnik, Fate of the false monopoles: Induced vacuum decay, Phys. Rev. D **82**, 025022 (2010).
[49] B.-H. Lee, W. Lee, R. MacKenzie, M. B. Paranjape, U. A. Yajnik, and D.-h. Yeom, Tunneling decay of false vortices, Phys. Rev. D **88**, 085031 (2013).
[50] A. R. Gomes, F. C. Simas, K. Z. Nobrega, and P. P. Avelino, False vacuum decay in kink scattering, J. High Energy Phys. 10 (2018) 192.

[51] P. Dorey, A. Gorina, I. Perapechka, T. Romańczukiewicz, and Y. Shnir, Resonance structures in kink-antikink collisions in a deformed sine-Gordon model, J. High Energy Phys. 09 (2021) 145.
[52] Here f_π is the pion decay constant and e is the Skyrme coupling; the parameters can be tuned to reproduce the masses of the neutron, the pions and the delta resonance, see, e.g., [17].
[53] I. Y. Kobzarev, L. B. Okun, and M. B. Voloshin, Bubbles in metastable vacuum, Yad. Fiz. **20**, 1229 (1974).
[54] S. R. Coleman, The fate of the false vacuum. 1. Semiclassical theory, Phys. Rev. D **15**, 2929 (1977); **16**, 1248(E) (1977).
[55] L. Ferreira and J. Guillén, Infinite symmetries in the Skyrme model, Phys. Lett. B **504**, 195 (2001).
[56] M. Hale, O. Schwindt, and T. Weidig, Simulated annealing for topological solitons, Phys. Rev. E **62**, 4333 (2000).
[57] N. S. Manton and B. M. A. G. Piette, Understanding skyrmions using rational maps, Progress of mathematics **201**, 469 (2001).
[58] D. Foster and N. S. Manton, Scattering of nucleons in the classical Skyrme model, Nucl. Phys. **B899**, 513 (2015).
[59] R. A. Battye, M. Haberichter, and S. Krusch, Classically isospinning Skyrmion solutions, Phys. Rev. D **90**, 125035 (2014).
[60] R. A. Battye and M. Haberichter, Isospinning baby Skyrmion solutions, Phys. Rev. D **88**, 125016 (2013).
[61] A. Halavanau and Y. Shnir, Isorotating baby Skyrmions, Phys. Rev. D **88**, 085028 (2013).
[62] A. Shkerin and S. Sibiryakov, Black hole induced false vacuum decay: The role of greybody factors, arXiv:2111.08017.
[63] J. A. Neto, A note in the Skyrme model with higher derivative terms, J. Phys. G **20**, 1527 (1994).
[64] I. Floratos and B. Piette, Multiskyrmion solutions for the sixth order Skyrme model, Phys. Rev. D **64**, 045009 (2001).